Effects of the body force on the pedestrian and evacuation dynamics

I.M. Sticco[a], G.A. Frank[b], C.O. Dorso[a,c,*]

[a]*Departamento de Física, Facultad de Ciencias Exactas y Naturales, Universidad de Buenos Aires, Pabellón I, Ciudad Universitaria, 1428 Buenos Aires, Argentina.*
[b]*Unidad de Investigación y Desarrollo de las Ingenierías, Universidad Tecnológica Nacional, Facultad Regional Buenos Aires, Av. Medrano 951, 1179 Buenos Aires, Argentina.*
[c]*Instituto de Física de Buenos Aires, Pabellón I, Ciudad Universitaria, 1428 Buenos Aires, Argentina.*

Abstract

The Social Force Model (SFM) is a suitable model for describing crowds behaviors. In this research, we analyze the role of the body force in the original SFM. We focus on the parameter associated with the body stiffness (k_n) and its impact on the pedestrian dynamics in two different geometries: bottleneck and corridor. Increasing k_n produces opposite effects depending on the geometry analyzed. Pedestrians move faster in a bottleneck, but they move slower in corridors as k_n increases. The improvement in the bottleneck geometry is because increasing the stiffness reduces the contacts among pedestrians. This effect reduces the number of blocking clusters close to the exit door (which is critical to improving the evacuation). The slow down in the corridor geometry occurs because when k_n increases, the crowd behaves like a solid-granular-system in which the friction interaction with the wall determines the velocity of the whole crowd. We have also explored the dimensionless parameters that arise from the reduced-in-units equation of motion and tune them to reproduce the qualitative behavior of the empirical fundamental diagram.

Keywords:
Pedestrian Dynamics, Social Force Model, Body Force

*codorso@df.uba.ar

PACS: 45.70.Vn, 89.65.Lm

1. Introduction

The Social Force Model (SFM) models the crowd dynamics considering three kinds of force: desired forces, social forces, and physical forces. In its original version, the SFM, addresses two physical forces as essential: the "body force" and the "sliding friction". Both are inspired by granular interactions and were claimed to be necessary for attaining the particular effects in panicking crowds [1]. The "sliding friction" actually proved to be an essential feature of the "faster-is-slower" effect, although the role of the "body force" appears, at a first instance, not so clear [2, 3, 4].

The existence of a "body force" in the context of highly dense crowds (say, 5 to 10 people/m^2) is a commonsense matter [5, 6]. Researchers, however, question the numerical setting for this force in the SFM context [7]. As a matter of fact, the usual setting by Helbing prevents the excessive overlapping among pedestrians, but it is known to accomplish artificially high force levels [1, 7, 8, 9]. The force estimates from the SFM appear to be remarkably higher with respect to the reported real life data (say, an order of magnitude). The crowd motion simulations, however, present quite realistic results [7, 8, 10]. The point seems to be that the SFM focuses on the "collective behavior" due to clogging, missing the "individualistic" perspective of single pedestrians or very small groups [1, 5, 11].

Many researchers realized that modifying the SFM may (partially) surpass the misleading parameter setting. It was proposed that the pedestrians' psychological force (say, the "social force") should be suppressed in the context of highly dense crowds [12, 13, 14, 15], or smoothly quenched according to the crowd density [16]. The authors in Refs. [17, 18] further proposed a rigid body model in order to completely avoid the overlapping phenomenon. This perspective dismisses any connection to a "sliding friction". Conversely, other authors tried to limit the pedestrians acceleration by introducing "static friction" between the pedestrians and the floor [19]. This kind of friction, however, reduces the effective willings of the pedestrians.

A unique (and universal) setting appears not available yet to our knowledge. The reason is that different numerical settings can lead to the same

crowd dynamics. Actually, only a small set of dimensionless "numbers" control the crowd dynamics [20]. These are similar to those encountered in other active matter systems (Péclet number, etc.) [21]. We may hypothesize that while the dimensionless "numbers" provide some kind of control on the collective behavior in crowds, only a few numerical settings can attain an "individualistic" meaning.

The numerical setting for the "faster is slower" effect presented by Helbing and co-workers is somewhat cumbersome Ref. [1, 10, 20]. Although a single parameter (say, the desired velocity v_d) is numerically varied to explain the phenomenon, the researcher looses sight of the dimensionless "numbers" that truly control the crowd dynamics. The setting in Ref. [1] also misses the "faster is faster" effect reported to occur at very high pedestrian densities [10, 22]. Alternatively, the empirical fundamental diagram raises as a point of reference for the SFM control parameters [23, 10].

The fundamental diagram exhibits the flux behavior for either low dense crowds (with seldom contacts between pedestrians) and highly dense crowds (dominated by body forces and sliding friction). The latter usually experiences a flux slowing down, but other behaviors are also possible [23, 24]. In light of our previous hypothesis, we may suspect that the modeling of the "flux slowing down" within the context of the SFM will require the proper setting of the (dimensionless) controlling parameters. We examined this working hypothesis in Ref. [20], but limiting the parameter exploration to the sliding friction, disregarding the body force.

We now widen the investigation on the parameter settings to include the one associated to the body force. We will explore the complex interplay between the body force and the sliding friction among pedestrians. Recall that the interplay dynamics is not directly controlled by the numerical setting, but through dimensionless "numbers", where the model parameters appear mixed between each other. Thus, this step up offers a challenge to the "individualistic" meaning of the parameter's setting.

The investigation is organized as follows. We first recall the available experimental values on the body force and the sliding friction (see Section 2). Secondly, we introduce the reduced-in-units SFM and the three dimensionless numbers that control the crowd dynamics (see Section 3). We present our

numerical simulations in Section 5. For the sake of clarity, this Section is separated into two major parts: the bottleneck scenario and the corridor scenario in Sections 5.1 and 5.2, respectively. Section 6 opens a detailed discussion from results in Section 5 and resumes our main conclusions.

2. Experimental background

The complex behavior of pedestrians features either his (her) feelings and the environmental conditions. The former is expressed, for example, by his (her) moving "attitude" (say, self-assuredness). The latter brings out the observed separation between pedestrians. Also, the "contacts" between individuals address some kind of "unwanted" slowing down. All these observed patterns are commonly quantified in the literature into a set of characteristic parameters. The experimental meaning of these parameters is as follows.

(i) The walking attitude of a pedestrian may appear somewhat "aggressive" if he (she) reacts actively to unexpected behaviors [7, 25]. The smaller the reaction time, the more aggressive observed posture. The associated parameter to this behavior is the relaxation or characteristic time τ [26, 1].

(ii) Despite the reactive attitude τ, the pedestrian addresses a "free" (undisturbed) walking speed v_d. This speed expresses his (her) motivation or intention to reach a certain destination (as comfortable as possible). Observations commonly associate $0.6\,\mathrm{m/s}$, $1\,\mathrm{m/s}$ or $1.5\,\mathrm{m/s}$ to relaxed, normal or nervous walking speeds, respectively [25, 1, 27].

(iii) The walking speed of pedestrians appears to be lower in a crowded walkway with respect to their usually expected "free" walking speeds [28, 7]. Pedestrians tend to reduce their speed within crowded environments because they perceive not enough space for taking a step [26]. This (perceived) step distance is therefore an influential parameter on the pedestrians behavior. It is known as the characteristic length B.

(iv) Physical interactions occur in very crowded environments. The "body force" and "sliding friction" can be introduced straight forward. This will be done in Section 3. But it is worth noting that both are associated to the moving difficulties (say, slowing down and obstructions) observed in contacting pedestrians.

τ[s]	m[kg]	v_d[m/s]	B[m]	k_n[kg/s^2]	Refs.
0.61	—	1.24	$0.36 + 1.06\,v$	—	[30]
0.50*	80*	1.34	0.50	—	[28, 7]
—	67.5	1.39	—	$96.1 + 12694.1\,x$	[16]
—	67.0	1.39	—	$97.0 + 29378.9\,x$	[16]

Table 1: The experimental data for the pedestrian parameters, as explained in Section 2. The magnitude v means the actual pedestrian velocity (m/s). The magnitude x means the compression length (m). The upper row for Ref. [16] corresponds to data acquired in winter and the lower row to data acquired in summer. The asterisk (*) corresponds to reasonable estimates from the authors.

Table 1 shows a few empirical values for the most common parameters. More data is available throughout the literature (see, for example, Refs. [29, 30, 31, 32, 33, 34, 27]). We intentionally omitted data that assumes a specific mathematical model. The exhibited values should also be considered as a general purpose approach, since no distinction has been made on age, gender or cultural habits.

A first examination of the figures in Table 1 shows that the choice $\tau \simeq 0.6\,\mathrm{s}$ seems to be a reasonable estimation for the relaxation time, although this may vary with respect to gender or culture [35]. Additionally, we confirm that normal pedestrians attain desired velocities around $1.3\,\mathrm{m/s}$.

The reports from Refs. [30, 28] do not include any values for the compressibility k_n since these experiments were carried out under low density conditions. The minimum (perceived) step distance is $0.36\,\mathrm{m}$ according to Ref. [30], but the pedestrians seem to require larger distances when they walk faster. The commonly accepted value $B \simeq 0.5\,\mathrm{m}$ is somewhat valid for walking speeds under $0.5\,\mathrm{m/s}$ [30]. Higher walking speeds (say, $1\,\mathrm{m/s}$) will require a step distance of $1.3\,\mathrm{m}$ for the pedestrians to feel that there is enough space to move along.

The reported data from Ref. [16] correspond to the crowded environment of the Beijing subway. This environment was not suitable for providing information on the step distance B, but estimates for the desired speed and the body compressibility could be achieved. The reported magnitude k_n assesses either the clothes and the body compressibility. The final value, though, is

linearly related to the compression x.

We measured the maximum attainable forces during the spring of 2019 at the subway in Buenos Aires, Argentina. Our preliminary results show that pedestrians feel "uncomfortable" whenever a body force ranging from 5 to 20 N is applied for at least ten minutes. Short lasting forces (say, less than 4 minutes) may also be perceived as "uncomfortable" for values ranging from 10 to 30 N. We also recorded body forces up to 60 N during very short "hits". The comparison with the fittings provided by Ref. [16] shows that these magnitudes accomplish densities around 5 people/m^2.

The maximum (realistic) compressions may be computed from the hook relation $F(x) = k_n(x)\, x$ and the compressibility $k_n(x)$ reported in Table 1. An "uncomfortable" body force $10\,\mathrm{N} - 30\,\mathrm{N}$ can address compressions in the range of $0.030 - 0.055\,\mathrm{m}$. Also, a "hitting" force of 60 N can address compressions between 0.045 and 0.065 m. Thus, according to Table 1, we may expect experimental values for $k_n(x)$ up to $1000\,\mathrm{kg/s^2}$ (for $F = 30\,\mathrm{N}$), or, up to $1400\,\mathrm{kg/s^2}$ (for $F = 60\,\mathrm{N}$).

Besides, no reliable values for the sliding friction κ appears to be available in the literature (to our knowledge). We may presume, however, that the sliding friction approaches a fraction of the body force. We will come back to this issue in Section 3.

3. Theoretical background

3.1. The Social Force Model

The Social Force Model (SFM) provides the necessary framework for simulating the collective dynamics of self-driven particles (*i.e.* pedestrians). The pedestrians are considered to follow an equation of motion involving either "socio-psychological" forces and physical forces (say, granular forces). The equation of motion for any pedestrian i (of mass m_i) reads

$$m_i \frac{d\mathbf{v}_i}{dt} = \mathbf{f}_d^{(i)} + \sum_{j=1}^{N} \mathbf{f}_s^{(ij)} + \sum_{j=1}^{N} \mathbf{f}_g^{(ij)} \tag{1}$$

where the subscript j corrresponds to any neighboring pedestrian or the walls. The three forces $\mathbf{f}_d$, $\mathbf{f}_s$ and $\mathbf{f}_g$ are different in nature. The desire force $\mathbf{f}_d$ represents the acceleration (or deceleration) of the pedestrian due to his (her) own willings. The social force $\mathbf{f}_s$, instead, describes the tendency of the pedestrians to stay away from each other. The granular force $\mathbf{f}_g$ stands for either the sliding friction and the compression between pedestrians.

Notice that these forces are supposed to influence the behavior of the pedestrians in a similar fashion as mentioned in Section 2. Thus, the set of (empirical) parameters described in Section 2 is expected to be also present in the SFM. These will appear in connection to the forces, although their meaning may be somewhat different.

The pedestrians' own willing is modeled by the desire force $\mathbf{f}_d$. This force stands for the acceleration (deceleration) required to reach a certain position at the desired walking speed v_d. This involves, however, a personal attitude that makes him (her) appear more or less "assertive". As mentioned in Section 2, the reaction time τ attains for this attitude. Thus, the desire force is modeled as follows

$$\mathbf{f}_d^{(i)} = m\,\frac{v_d^{(i)}\,\hat{\mathbf{e}}_d^{(i)}(t) - \mathbf{v}^{(i)}(t)}{\tau} \tag{2}$$

where $\hat{\mathbf{e}}(t)$ represents the unit vector pointing to the target position. $\mathbf{v}(t)$ stands for the pedestrian velocity at time t.

The tendency of any individual to preserve his (her) "private sphere" is accomplished by the social force $\mathbf{f}_s$. This force is expected to prevent the pedestrians from getting too close to each other (or to the walls) in a crowded environment. If he (she) perceives that there is not enough space to move, he (she) will decelerate or even move back. The model for this kind of "socio-psychological" behavior is as follows

$$\mathbf{f}_s^{(i)} = A\,e^{(R_{ij}-r_{ij})/B}\,\hat{\mathbf{n}}_{ij} \tag{3}$$

where r_{ij} means the distance between the center of mass of the pedestrians i and j, and $R_{ij} = R_i + R_j$ is the sum of the pedestrians radius. The unit vector $\hat{\mathbf{n}}_{ij}$ points from pedestrian j to pedestrian i, meaning a repulsive interaction.

The net distance (overlap) $|R_{ij} - r_{ij}|$ scales to the parameter B in the expression (3). This parameter plays the role of a fall-off length within the model, and thus, it may be somewhat connected to the (perceived) step distance mentioned in Section 2. The parameter A, however, does not provide any direct link to other parameters mentioned there.

The granular force (say, the sliding friction plus the body force) attain to the moving difficulties encountered in very crowded environments. The expression for the granular force is has been borrowed from other granular matter fields, as follows

$$\mathbf{f}_g^{(ij)} = \kappa\, g(R_{ij} - r_{ij})\, (\Delta \mathbf{v}^{(ij)} \cdot \hat{\mathbf{t}}_{ij})\, \hat{\mathbf{t}}_{ij} + k\, g(R_{ij} - r_{ij})\ \hat{\mathbf{n}}_{ij} \tag{4}$$

where $g(R_{ij} - r_{ij})$ equals $R_{ij} - r_{ij}$ if $R_{ij} > r_{ij}$ and vanished otherwise. $\Delta \mathbf{v}^{(ij)} \cdot \hat{\mathbf{t}}_{ij}$ represents the difference between the tangential velocities of the sliding bodies (or between the individual and the walls).

The sliding friction occurs in the tangential direction while the body force occurs in the normal direction. Both are assumed to be linear with respect to the net distance between contacting pedestrians. The sliding friction is also linearly related to the difference between the (tangential) velocities. The coefficients κ (for the sliding friction) and k_n (for the body force) are supposed to be related to the areas of contact and the clothes material, among others.

We stress that the expression (4) assumes fixed values for κ and k_n. This may not be completely true according to Table 1. The local density (and thus, the pedestrians' compression) may affect the compressibility parameter k_n by more than an order of magnitude. We will vary k_n (and κ) in order to explore this phenomenon.

3.2. The parameters setting

The numerical setting of the parameters may affect the dynamics of the pedestrians. Some settings, however, yield similar collective dynamics. We introduce unit-less magnitudes and proceed straightforward as indicated in Appendix A. We realize from Appendix A that only three (unit-less) parameters are the true "control" parameters for the collective dynamics. These

are $\mathcal{A}$, $\mathcal{K}$, $\mathcal{K}_c$ as defined in Appendix A. Recall that $\mathcal{A}$ and $\mathcal{K}$ are precisely the same as in Ref. [20], but a novel $\mathcal{K}_c$ parameter has been introduced due to the body force.

The logical relations between the unit-less parameters and the "individual" parameters can be studied by means of the Venn diagrams exhibited in Fig. 1. The parameters $\mathcal{A}$, $\mathcal{K}$ and $\mathcal{K}_c$ are represented as intersecting sets, and the "individual" parameters are represented as elements within each set. The shared elements between $\mathcal{A}$, $\mathcal{K}$ and $\mathcal{K}_c$ are placed inside the intersecting regions.

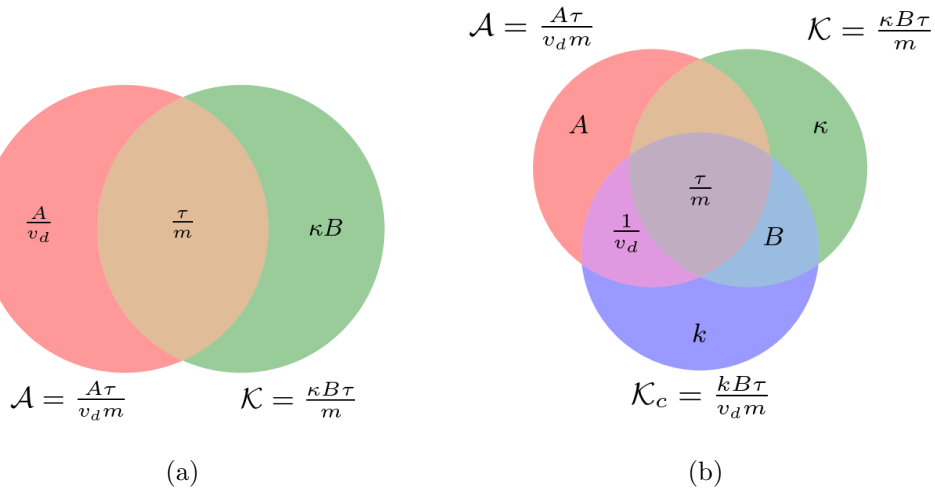

Figure 1: Venn diagrams for the unit-less parameters appearing in the equation of motion (1) (see Appendix Appendix A for details). The sets correspond to $\mathcal{A} = \{\tau/m, 1/v_d, A\}$, $\mathcal{K} = \{\tau/m, B, \kappa\}$ and $\mathcal{K}_c = \{\tau/m, 1/v_d, B, k\}$. (a) The Venn diagram representation if no body force is introduced in the SFM (only sets $\mathcal{A}$ and $\mathcal{K}$, as in Ref. [20]). (b) The Venn diagram representation for the sets $\mathcal{A}$, $\mathcal{K}$ and $\mathcal{K}_c$.

A first inspection of the diagrams in Fig. 1 shows that the relaxation time (per unit mass) τ/m is always a common parameter to all sets, regardless of the body force. This means that the "assertive" attitude of the pedestrian, addressed by the reaction time (see Section 2), applies to all stimuli and the own willings. The role of τ has already been discussed in Refs. [26, 20].

Fig. 1a represents the situation when $\mathcal{K}_c$ is absent. Notice that A/v_d or

κB may control the collective dynamic, in spite of the "assertive" attitude. The individual character of v_d or B appears somehow "loosely" in the crowd dynamic. We mean by "loosely" that any numerical setting of these parameters may be counterbalanced by the right setting of A or κ, keeping the colletive dynamic (qualitatively) unchanged.

Fig. 1b provides a picture of the parameters' relations after introducing $\mathcal{K}_c$. Surprisingly, $\mathcal{K}_c$ appears as a wider set (say, a four elements set) than $\mathcal{A}$ or $\mathcal{K}$ (three elements' sets). It shares the parameter v_d with $\mathcal{A}$ and the parameter B with $\mathcal{K}$. The practical consequence to these (logical) relations is that v_d or B affect simultaneously two "control" parameters of the collective dynamics. Conversely, either v_d and B may counterbalance $\mathcal{K}_c$ in order to keep the colletive dynamic (qualitatively) unchanged.

We confirm from these diagrams that no univocal relations can be established between the individual parameters and the collective dynamics (in a crowded environment). The presence of the body force moves the dynamics to a more complex context. We will investigate this context in section 5.

4. Working hypotheses and procedures

4.1. Working hypotheses

Our working hypotheses are similar to those mentioned in Ref. [20], although the presence of the body force opens inquiries about the proper exploration of the parameter space. To be precise

(a) The "faster-is-slower" (or the "faster-is-faster") phenomenon occurs when varying the values of v_d (see Section 5.1). This is equivalent to vary simultaneously $\mathcal{A}$ and $\mathcal{K}_c$ by the same amount in the (unit-less) parameter space (see Section 3.2). We may visualize this sampling procedure as moving along a straight line in the space $(\mathcal{A}, \mathcal{K}, \mathcal{K}_c)$. Further variations of k_n turns the sample points out of this line, but on the plane of constant $\mathcal{K}_c$. We will step up k_n by several orders of magnitude in order to get the big picture of this surface.

(b) We will consider the parameter setting in Ref. [1] as a starting point for exploring the parameter space. The reason for this is that a com-

plete set of experimental parameters is still not available (to our konwledge). We are aware, though, of the drawbacks for this choise, say, the unrealistic meanings for the length B and the compressibility k_n (see Section 2). But these are irrelevant in the context of the (unitless) parameter space and the corresponding collective dynamics (see Section 1).

(c) We will explore crowd densities allowing body compressions up to 0.1 m. This corresponds to remarkably high densities, since our own (real-life) estimates do not surpass 0.065 m (see Section 2). Therefore, the extremely high density scenarios (say, above 0.065 m) will be considered for the purpose of a tendency, but not as a common real-life situation. No casualties due to high pressures will be further considered.

We stress the fact that our concern is placed on the collective dynamics of crowded environments. We will work on the hypothesis that any "reasonable" parameter set should reproduce the collective behavior (say, the slowing down in the fundamental diagram; see Section 5.2). We will not attempt to optimize parameters from other objective functions.

We will further sustain the hypothesis of soft matter in the context of crowded environments. The body compression and the sliding friction parameters are supposed to be connected in some way under this hypothesis. However, we will not introduce any direct link between $\mathcal{K}$ and $\mathcal{K}_c$. We will investigate the interplay between both in Section 5.2.

In order to keep the model as simple as possible, we will only consider isothropic pedestrians, since anisothropy does not play a relevant role at high densities.

4.2. Procedures

The SFM was implemented on the LAMMPS simulation software [39]. Additional modules for LAMMPS were also written in C++ in order to expand the software capabilities. All these were able to run in a high performance environment (HPC).

The implemented SFM parameters were the same as those in Ref. [1] (at the begining of the exploratory procedure only). But the pedestrian's mass

and radius were set to the more realistic values of 70 kg and 0.2 m, respectively. The force interaccions between pedestrians were limited, however, to a cut-off distance of 0.88 m for attaining a *privacy sphere* from first neighbors only. The desired velcity was always set to 1 m/s in the corridor situation. Besides, the explored values of v_d for the bottleneck scenario ranged from 1 m/s to the extremely anxious situation of 10 m/s.

The Eq. (1) was numerically integrated by means of the velocity Verlet algorithm, with a timestep of 10^{-4} seconds. The pedestrians positions and velocities were recorded every 0.05 sec, but post-processing computing was done over samples acquired every 5 sec., in order to avoid data correlations. Those pedestrians leaving the simulations box were re-introduced into the box, on the opposite side (periodic boundary conditions). We only ommitted this mechamism when computing the evacuation time for the bottleneck geometry.

The post-processing computing was assisted by Python functions. The NetworkX package was used among others.

5. Results

5.1. Bottleneck

We present in this section the results corresponding to the bottleneck geometry. We show the consequences of modifying the body force coefficient k_n in the evacuation dynamics. Recall that this coefficient is associated to the compression of the human body.

Fig. 2 shows the evacuation time as a function of the pedestrian's desired velocity for different values of k_n. The evacuation time is defined as the time until 80% of the pedestrians have left the room. In this section we will focus on the evacuation time for 2 m/s$< v_d <$ 10 m/s.

Two behavioral patterns can be seen in Fig. 2. The region in which the slope is positive means that the harder the pedestrians try to get out (higher v_d), the longer it takes them to evacuate. This is the Faster-is-slower (FIS) regime. Conversely, the region in which the slope is negative corresponds to a Faster-is-Faster (FIF) regime (the harder they try, the quicker they leave).

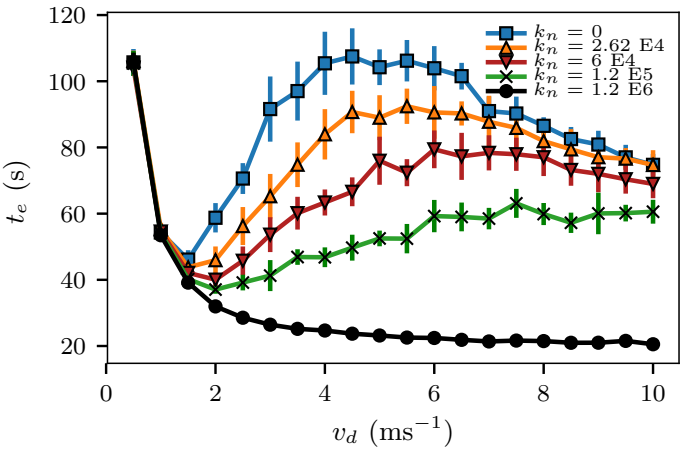

Figure 2: Mean evacuation time (s) vs. the pedestrians desired velocity (m/s) for a bottleneck. The room was 20 m x 20 m size. The door was 0.92 m width. Mean values were computed from 10 evacuation processes. 225 pedestrians were initially placed in a square lattice with a random initial velocity. Each process was finished when 158 pedestrians left the room. The different symbols indicate the k_n value corresponding to the body force (see the label). The crosses correspond to the Helbing's original SFM parameter, the up-triangles correspond to the value measured in Ref. [37], squares correspond to zero body force and circles correspond to an extreme value of stiffness (one order of magnitude higher than the original SFM). The down triangles correspond to an intermediate value between the empirical value presented in Ref. [37] and the chosen by Helbing in Ref. [1]

Fig. 2 shows a change in in the behavior for desired velocities $v_d > 1.2\,\mathrm{m/s}$. The evacuation time is of type FIS+FIF for compression coefficients below $k = 1.2\,\mathrm{E5}$. This means that "soft" individuals are required to attain this behavioral change. Notice that higher values of k_n allow only FIS or FIF behaviors. For the highest explored value $k_n = 1.2\,\mathrm{E6}$, no FIS can be seen at all. Besides, the evacuation pattern for $k_n = 0$ and $k_n = 1.2\,\mathrm{E4}$ are very similar since the body force is comparable to the social force for these stiffness values.

Despite the presence of the FIS or FIF phenomenon, the evacuation time at a fixed value of v_d decreases for increasing values of k_n. This means that stiffer pedestrians evacuate faster than soft pedestrians. To investigate this issue, we computed the mean velocity of the whole crowd as a function of the stiffens k_n. Fig. 3 shows the mean velocity in the x-direction as a function of the stiffness k_n for three different desired velocities. In all cases, the velocity increases with the stiffness. From $k_n = 0$ to k_n =1.2 E4 the increment of velocity is not as significative as it is for higher k_n.

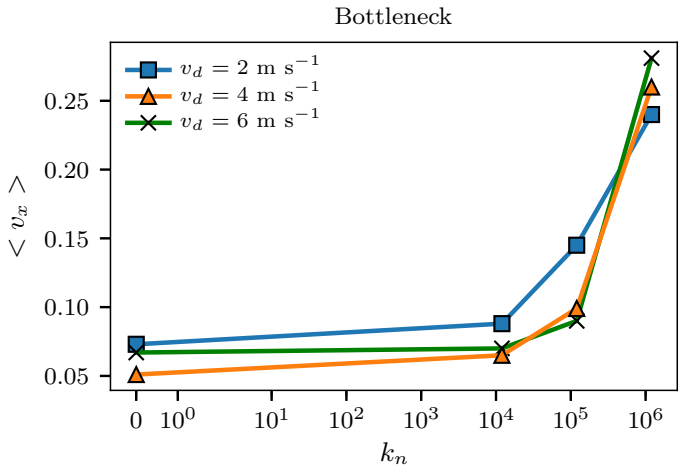

(a)

Figure 3: Mean velocity in the x-direction as a function of the stiffness level k_n for different desired velocities (see label). The data corresponds to a bottleneck with periodic boundary conditions (re-injecting pedestrians). The average was taken every two seconds once the crowd reaches the stationary state (t =20 s) until the end of the simulation (t =110 s).

The presence of a FIF phenomenon only for soft individuals opens many

questions on the microscopic dynamics of pedestrians. We may presume that contacts between pedestrians are quite different for soft individuals than for stiff individuals. To study the dynamics of the contact, regardless of the compression effects, we assimilate the pedestrians as nodes and the whole crowd as a network. We set a link between any two individuals if both are in physical contact (*i.e.* $r_{ij} \leq Rij$).

Fig. 4a shows the mean degree of the contact network as a function of the desired velocity. The degree of a node is defined as the number of links that connect this node to any other node. This means, the number of pedestrians that are in physical contact with a given pedestrian. The mean degree is the average of the degree over all the nodes (pedestrians) and over the whole sampled time. We report mean values after the system has reached the stationary state, that is after a well-formed bulk has been established.

Increasing v_d increases the mean degree, as expected. This occurs because increasing v_d produces higher densities that force individuals to touch each other. But surprisingly, for a given v_d, the mean degree reduces as the k_n value increases. A noticeable decrease in the mean degree can be seen for the highest explored value of k_n. We may expect a significant change in the sliding friction due to this fact.

A more detailed insight into the contact dynamics can be acquired from Fig. 4b. The overlap between individuals is shown as a function of v_d. Recall from section 3.1 that the overlap is defined as $R_{ij} - r_{ij}$ where R_{ij}, is the sum of radius of particle i and particle j and r_{ij} is the distance between both particles. Except for very low desired velocities (say, $v_d < 2\,\mathrm{m/s}$), we can see that the mean overlap is an increasing function of v_d (for the studied k_n values).

The regime for $v_d < 2\,\mathrm{m/s}$ is different from the rest since most of the pedestrians are not touching each other. The only pedestrians who touch each other are the ones who are being re-injected in the room. The overlap is higher than, for example, $v_d = 3\,\mathrm{m/s}$ because of the pedestrians that are re-injected and collide with pedestrians in the bulk.

Besides, for a given v_d, the overlap increases as the k_n value decreases. Reducing k_n means reducing the normal body force, which allows a more sig-

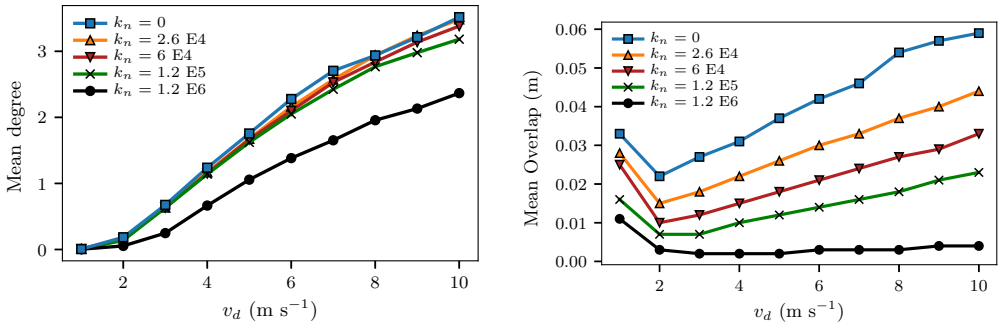

(a) (b)

Figure 4: (a) Mean degree as a function of the pedestrians desired velocity (m/s). (b) Mean overlap as a function of the pedestrians desired velocity. Each symbol indicates the k_n value corresponding to the body force (see the labels). The data corresponds to a bottleneck with periodic boundary conditions (re-injecting pedestrians). The average was taken every two seconds once the crowd reaches the stationary state (t =20 s) until the end of the simulation (t =110 s).

nificant intrusion of the personal space of the individuals (this means more overlap between pedestrians).

Increasing the body stiffness has a significant impact on evacuation dynamics. The reduction of the overlap and the mean degree between pedestrians in the simulation, tend to diminish the sliding friction within the crowd. Consequently, an enhancement in the evacuation time (pedestrians escape faster) is observed, as pictured in Fig. 2. Notice, however, that switching from a FIS regime (positive slope) to a FIF regime (negative slope) in Fig. 2 appears as a more complex phenomenon. We will focus on this issue in an upcoming investigation.

Despite the effects on the sliding friction, the body force has a notorious impact in the number of pedestrians touching each other (say, the degree). This is clearly depicted in Fig. 5 where four different configurations of the evacuation dynamics are shown. The configurations represent 225 pedestrians trying to escape through a door see the caption for details. The colors correspond to the degree of each node (pedestrian), and the lines between pedestrians represent the contacts among them.

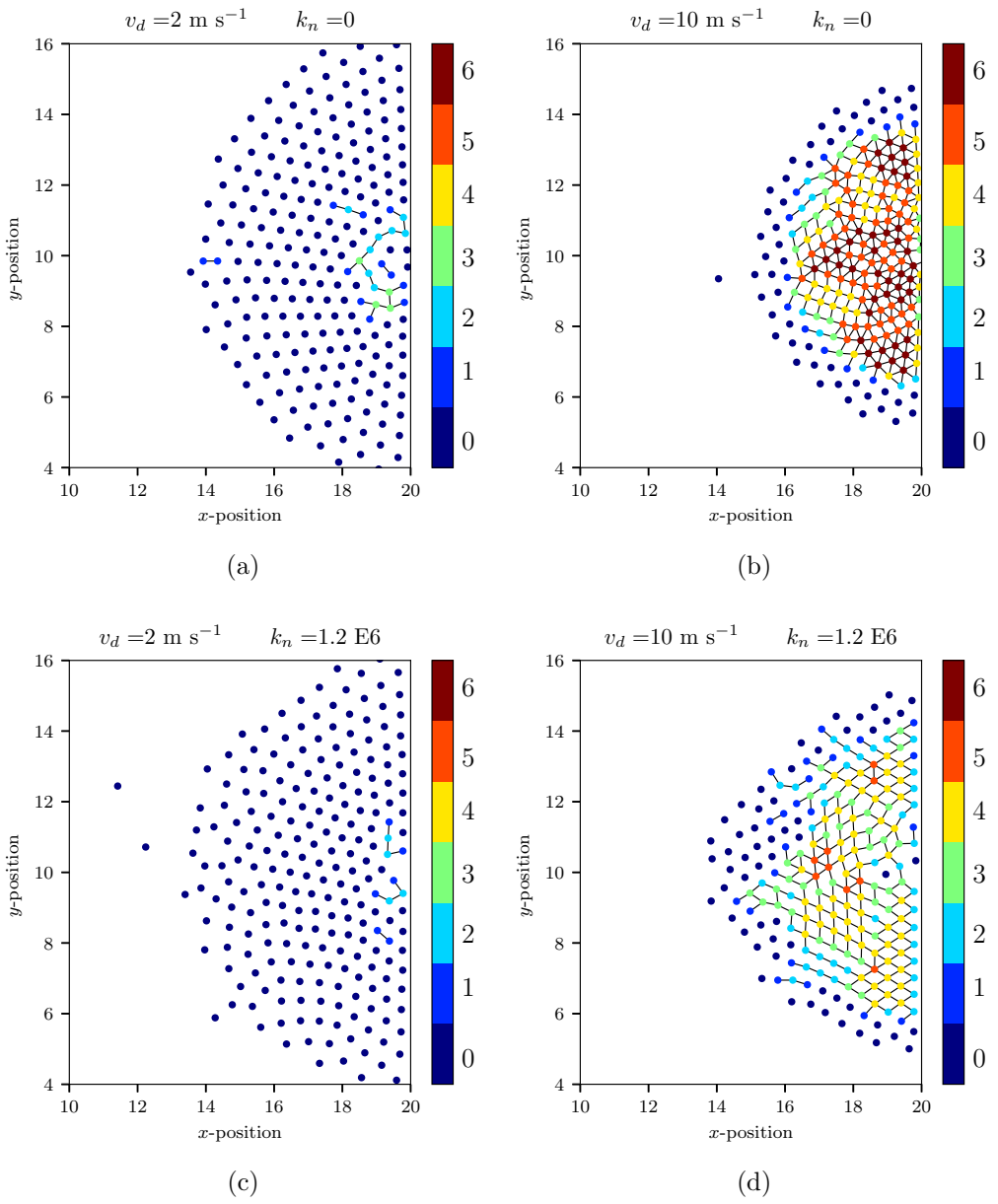

Figure 5: Contact networks of a 225 pedestrian evacuation through a bottleneck. The door is placed at $(x, y) = (20, 10)$ m, the width of the door is 0.92 m (equivalent to 2 pedestrian's diameter). The lines that connect the nodes (pedestrians) represent the contact between them. The color represents the degree (the number of pedestrians with which it is connected). (a) and (b) correspond to a simulation without body force with v_d =2 and v_d =10 respectively. (c) and (d) correspond to simulations with k_n=1.2 E6 with v_d =2 and v_d =10 respectively.

The four configurations corresponds to two different v_d and two different k_n values (say, the minimum and maximum explored values). Fig. 5a and Fig. 5b shows a snapshot for k_n =0, at desired velocities of 2 m/s and 10 m/s respectively. Fig. 5c and Fig. 5d show similar situations, but for k_n =1.2 E6. As expected, increasing the desired velocity compresses the crowd towards the exit.

The four snapshots in Fig. 5 confirm (visually) the fact that more rigid pedestrians release the crowded environment, widening the occupied region. At v_d = 10 m/s (the maximum explored velocity), it can hardly be found pedestrians with degree 6 when k_n = 1.2 E6, while a lot of them are present for k_n=0.

The clusterization of the pedestrians has a significant impact on the blocking clusters (the group of pedestrians that clog the exit). Fig. 6 shows the blocking cluster existence probability as a function of the desired velocity for different k values. The blocking clusters occur more often when the desired velocity increases because increasing v_d increase the density in the area close to the exit. The most remarkable fact of Fig. 6 is that increasing the stiffness reduces the blocking cluster existence for a fixed value of v_d. Under these conditions, the blocking clusters strictly govern the evacuation dynamics [2]. Thus, increasing the stiffness reduces the blocking cluster existence, which improves the evacuation time.

To conclude this section, we want to emphasize that increasing body stiffness has a significant impact on the evacuation dynamics. The stiffer pedestrians are, the less they touch to each other (less degree and less overlap). This phenomenon yields a reduction of the existence of the blocking clusters, which reduces the overall evacuation time.

5.2. Corridor

In this section, we present the results corresponding to the corridor geometry. We show the effects of modifying the body force coefficient k_n in the dynamics.

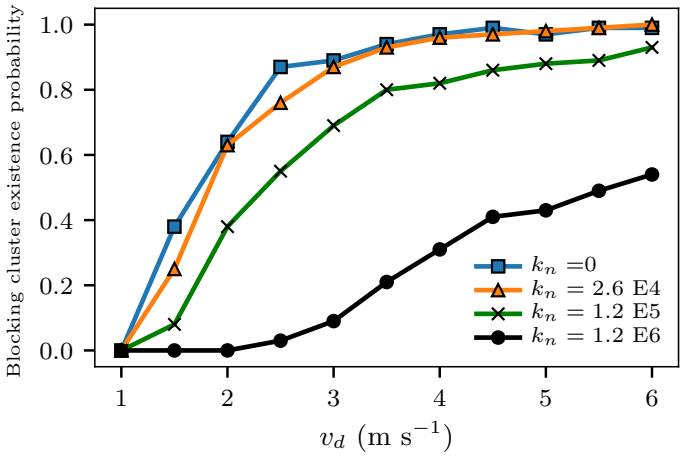

Figure 6: Blocking cluster existence probability as a function of v_d for different stiffness levels (see label). The probability is calculated as the amount of time a blocking cluster is present divided by the overall simulation time. The result correspond to a bottleneck geometry with 225 pedestrians in periodic boundary conditions (re-injection of pedestrians once the exited the room). The simulation lasted $t_f = 1000$ s.

In the same way as with the bottleneck geometry, we computed the contact network to study the topological differences that arise from increasing the k_n value. Fig. 7a shows the mean degree as a function of the global density for different k_n values. When the density is low, the degree is zero because the pedestrians do not touch each other. When the density is around 4.5, a few pedestrians start to touch each other increasing the mean degree. As the density increases, the mean degree increases until reaching an asymptotic behavior as approaching degree six. Degree six corresponds to the densest packing possible for identical hard circles; the result is a hexagonal packing arrangement.

It is important to notice that in Fig. 7a, for a given value of density, the stiffer the pedestrians, the higher the degree. In the bottleneck geometry, the opposite thing happens. The stiffer the pedestrians, the lower the mean degree.

The mean overlap increases as the global density increases (see Fig. 7b). For a given density, there is an inverse relation between stiffness and mean

overlap. This result is similar to the overlap vs. desired velocity obtained for bottleneck geometry. The higher the value of k_n, the higher the repulsion of the pedestrian-pedestrian interaction since the body force is acting on the direction n_{ij}.

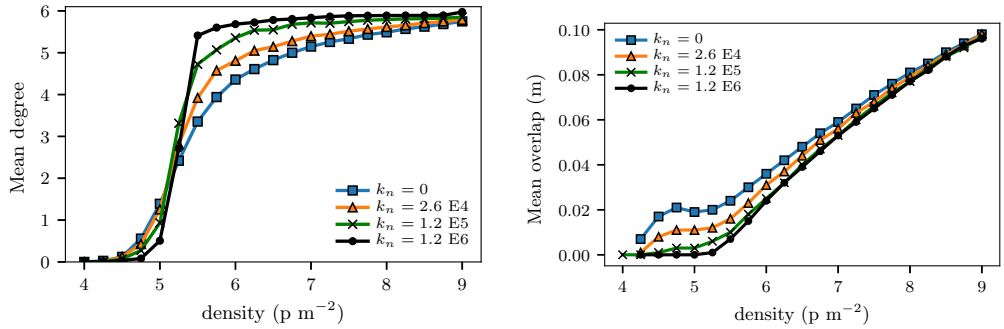

(a) (b)

Figure 7: (a) Mean degree as a function of the global density for different k_n values. (b) mean overlap as a function of the global density. The mean values are averages over all the pedestrians and over time once the system reaches the stationary state. Both measurements correspond to corridor geometry with desired velocity $v_d = 1$.

As was mentioned above, increasing the k_n value of the body force increases the stiffness of pedestrians. Increasing the stiffness reduces the overlap (both in the bottleneck and corridor). Regarding the network connectivity, increasing the stiffness reduces the mean degree in a bottleneck but increases the mean degree in a corridor. Fig. 8 shows the contact network corresponding to the corridor at a particular timestep ($t = 50$ s) and at a particular global density ($\rho = 7$). Fig. 8a corresponds to $k_n = 0$ while Fig. 8b corresponds to $k_n = 1.2$ E5. This is an example to show that increasing the stiffness increases the number of contacts between pedestrians (the network connectivity). Notice that there are many more pedestrians with degree 6 in the case of $k_n = 1.2$ E5 than the case of $k_n = 0$.

This result is exactly the opposite of what we get in the bottleneck geometry. This phenomenon occurs because, in the corridor, the lateral walls act like a containment barrier that forces the pedestrian to increase their contacts. Whereas in the bottleneck there are no lateral walls, thus, when increasing the stiffness they have more space to detach from each other, re-

ducing the connectedness (hence reducing the mean degree).

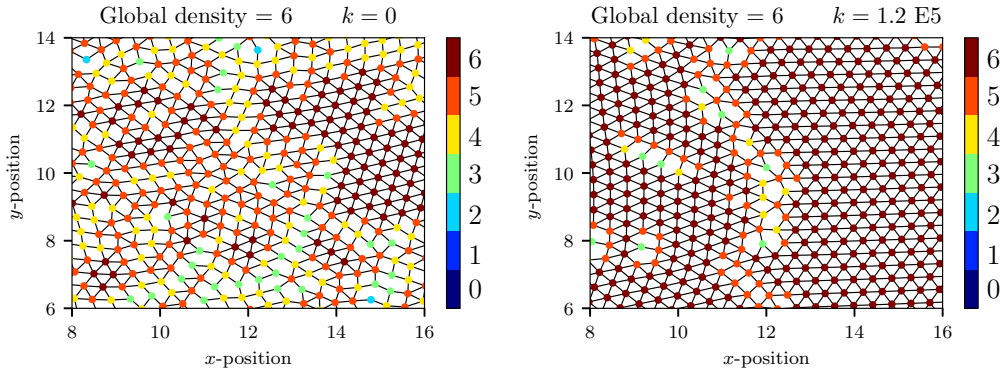

(a) (b)

Figure 8: Contact network of the pedestrians along the corridor. The lines that connect the nodes (pedestrians) represent the contact between them. The colors stand for the degree of the node (the number of pedestrians that are in contact with him/her). The corridor was 28 m $\times$ 22 m with periodic boundary conditions and $v_d = 1$. (a) corresponds to a simulation without body force and (b) corresponds to a simulation with $k_n = 1.2$ E5.

In the corridor geometry, the crowd gets more connected if the pedestrians become stiffer. We studied the network properties of the contact graph arising from the positions (x, y) of every pedestrian. We found that a good descriptor to exhibit the connectivity is the number of triangles per node. A triangle is defined as a structure composed of three nodes, all in contact with each other. Fig. 9 shows the triangles per node as a function of the global density for different stiffness values k_n. This descriptor allows distinguishing states with the same global density but different stiffness levels. In other words, it is a descriptor very sensitive to changes in stiffness that allow expressing the connectivity of the system even better than the mean degree.

This result is consistent with the results obtained in Ref. [36] where the authors explore several topological and geometrical descriptors capable of properly describing granular systems with different stiffness levels. While our study system is self-propelled, there are analogies with the system studied in Ref. [36]. Like the authors, we recommend using topological descriptors (in particular triangles per node) to describe systems with equal global density and different stiffness levels.

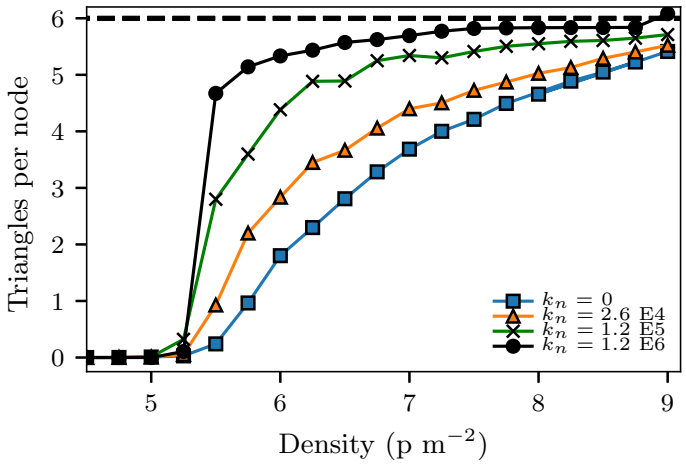

Figure 9: Triangles per node as a function of the global density. A triangle in a network is defined as three nodes all connected. Each marker corresponds to a different stiffness k_n (see the label in the plot). The measurements correspond to a corridor of 28 m $\times$ 22 m with periodic boundary conditions and $v_d = 1$.

The most important result is that increasing the k_n value reduces the flow (hence reduces the walking speed of the overall crowd) in the corridor geometry. Fig. 10 shows the mean velocity in the direction of displacement v_x as a function of the stiffness for different global density levels. v_x reduces as k_n increases as opposed to what happens in the bottleneck geometry. There is little to no change in the speed from zero to k_n =1.2 E4, from this value on, the diminishing of velocity is more abrupt.

The reason why the velocity reduces as the stiffness of the pedestrians' increases is that it becomes harder for pedestrians to walk forward. The difficulty arises because the pedestrian feels a much higher repulsion from the pedestrian ahead (due to the body force increment). Thus, they have no choice but to move at (almost) the same speed as the individuals they have at their sides. This microscopic mechanism explains the macroscopic behavior that turns the crowd from a "fluid-like state" into a "solid-like state". When the stiffness is high enough (say k_n =1.2 E6), all the pedestrians walk at the same velocity. The pedestrians that walk in physical contact with the wall

are the ones who determine the velocity of the whole crowd.

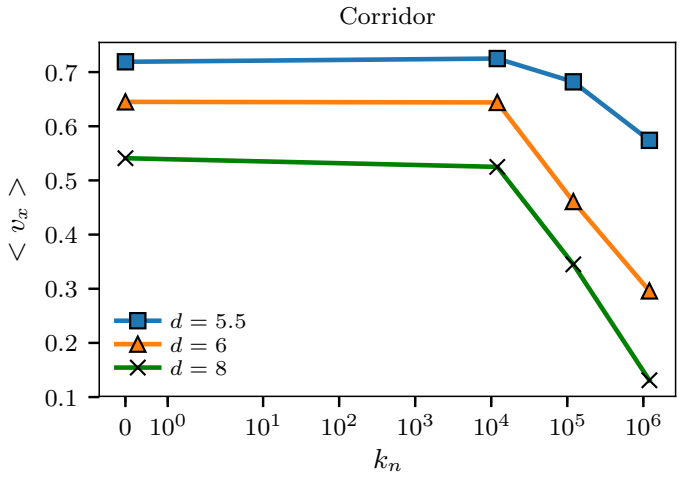

Figure 10: Mean velocity in the longitudinal coordinate (v_x) as a function of the stiffness k_n for three different global densities (see label in the plot). The measurements correspond to a corridor of 28 m $\times$ 22 m with periodic boundary conditions and $v_d = 1$.

The value of k_n affects the velocity all along the corridor. Fig. 11a shows the velocity profile (v_x vs. the longitudinal coordinate y) for different k_n values. For $k_n = 0$, we can see a parabolic-like velocity profile that resembles the Poiseuille flow (for Newtonian and incompressible fluids in laminar flow flowing through a pipe). This behavior was observed in empirical measurements reported in Ref. [38]. As k_n increases the velocity profile flattens until becoming a constant (k_n = 1.2 E6). In this scenario, the value of mean v_x is much lower than on the case of soft pedestrians (k_n =0).

If the stiffness is high enough, the crowd behaves like a solid; this means that the crowd can not be easily "deformed". In this context, to deform means to have certain parts of the crowd that manage to move faster than other parts of the crowd.

The strain rate is a tensor for every point in the space. It expresses how the relative velocity of a medium changes when one moves away from a position in a specific direction. For this particular problem, we define the

following version of the strain rate:

$$S = \frac{< v_x(center) > - < v_x(boundary) >}{|y(center) - y(boundary)|} \tag{5}$$

Where <> means the average taken over time. By this definition we compare the velocity of the pedestrians close to the wall (boundary) with respect to the velocity of the pedestrians in the center of the corridor (center). As the stiffness level increases, the crowd becomes less deformable. This phenomenon is shown in Fig. 11b where we can see that the strain rate decreases with k_n.

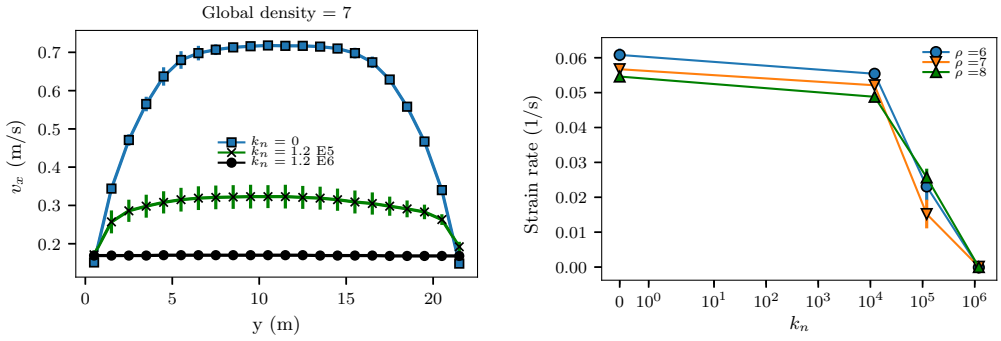

(a) (b)

Figure 11: (a) Velocity in the x coordinate as a function of the transversal coordinate y for three different stiffness values k (see the label). (b) Strain rate as a function of the stiffness level k_n for three different global density values (see label). The measurements correspond to a corridor of 28 m × 22 m with periodic boundary conditions and $v_d = 1$. The global density was 7 p m^{-2}.

To conclude section 5.2, we remark that increasing the stiffness produces the opposite results in corridors respect to bottlenecks. The walls in the corridors play a critical role that prevents pedestrians from detaching from each other. This effect has consequences such as increasing the connectivity of the contact network and flattening the velocity profile (thus reducing the strain rate). If the stiffness is high enough, the pedestrians can not push to the pedestrian ahead since the body force repulsion becomes very high. This leads to a "solidification" of the crowd that makes all the pedestrians walk at almost the same velocity. The pedestrians that are in contact with the

wall are the ones who determine the velocity of the whole crowd.

5.3. Dimensionless numbers and comparison with empirical data

In this section, we inspect different values of the dimensionless numbers $\mathcal{K}_c$ and $\mathcal{K}$ and compare the results with the empirical measurements of Ref. [23]. We varied the body force coefficient (k_c) and the friction coefficient (k_t) to inspect different values of $\mathcal{K}_c$ and $\mathcal{K}$ respectively.

The empirical measurements correspond to the fundamental diagram measured at the entrance of the Jamaraat bridge (see the inset in Fig. 12a). We aim to reproduce the qualitative behavior of these measurements roughly.

Figs. 12 show the flow as a function of the global density (fundamental diagram). Fig. 12a corresponds to $\mathcal{K}_c = 0$ (zero body force *i.e.* $k_n = 0$) while Fig. 12b corresponds to $\mathcal{K}_c$ =68 (which is the value of the original SFM with k_n=1.2 E5). Each curve correspond to a different friction value, hence different k_t value (see the caption).

According to most of the empirical measurements of the fundamental diagram, the flow decreases for high enough values of density because the crowd becomes jammed. Notice that the original friction (corresponding to $\mathcal{K}$ =137) does not produce a reduction of the flow when there is zero body force ($\mathcal{K}_c$ =0). Nevertheless, when the body force is included, and we remain the original friction (circles from Fig. 12b), the flow reduces in the range of densities from 5 p m^{-2} to 7 p m^{-2}; then increases for higher values of density.

When the dimensionless number associated with the friction is $\mathcal{K} = 685$, the friction is five times the original SFM value. In this scenario, the flow reduces for densities higher than 5 p m^{-2} in both cases (with body force and without body force). The main qualitative difference is that including the body force produces a subtle increment in the flow for densities higher than 7 p m^{-2} (orange curve from Fig. 12a).

When the dimensionless number associated to the friction is $\mathcal{K}$ =1371 (the friction is ten times the original SFM value), in this case, the flow reduces or remains constant when the density is higher than 5 p m^{-2} for both

cases (with $\mathcal{K}_c = 0$ and $\mathcal{K}_c = 68$).

It worth mentioning that the SFM contemplates the possibility of overlapping between pedestrians (unlike the models stated in Refs. [17, 18]). Despite this hard-to-interpret feature, the SFM can reproduce empirical behaviors of collective pedestrian dynamics.

These results suggest that although increasing $\mathcal{K}_c$ produces a reduction in the flow, it is necessary to increase $\mathcal{K}$ (for instance, increasing the friction coefficient k_t) to reproduce the reduction in the flow that characterizes the high-density regime. It is still a pending challenge to find the values of the dimensionless numbers that reproduce the qualitative behavior of the fundamental diagram, but this first approach narrows down the search.

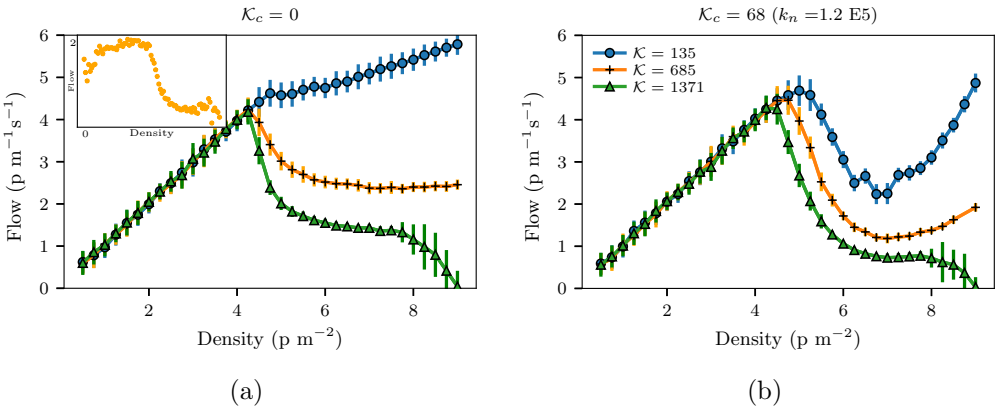

(a) (b)

Figure 12: Flow vs. global density. The flow is calculated in a circular area of R=1 m at the center of the corridor. The circular markers correspond to the original friction of the SFM, the "+" symbol corresponds to the friction increased by a factor of five and the triangles correspond to the friction increased by a factor of ten. The desired velocity was $v_d = 1$ in all the cases. (a) corresponds to simulations without body force ($\mathcal{K}_c$ =0) and (b) corresponds to a body force with the original value of the body stiffness ($\mathcal{K}_c$ =68).

6. Conclusions

In this research, we explore the effect on the pedestrians dynamics of the (sometimes neglected) body force in the framework of the SFM. We showed that the stiffness coefficient (k_n) has a significant impact on the evacuation

dynamics (bottleneck) and also in the dynamics of pedestrians walking along a straight corridor.

In the bottleneck geometry, the evacuation time diminishes (pedestrians move faster) as pedestrians become stiffer for all the ranges of the desired velocities explored. This phenomenon occurs because increasing the stiffness level promotes the repulsion between pedestrians pair interactions. As pedestrians detach from each other, the friction force diminishes due to the reduction of overlap between pedestrians and the contacts among them. The general decrease in frictional force reduces the probability of producing a cluster of pedestrians blocking the exit (blocking cluster), which leads to a more efficient evacuation dynamics.

In the corridor geometry, the actual walking speed reduces as pedestrians become stiffer. This is the opposite behavior with respect to the obtained in bottleneck geometry. The difference is explained because although increasing stiffness further separates individuals, they can not detach from each other as much as possible due to the lateral walls (these walls are not relevant in the bottleneck geometry). Thus, when the stiffness increases, the overlap between pedestrians is reduced while the number of contacts (degree) increases. Granular materials can behave like fluid or solids, depending on several conditions. If the stiffness level is low, the entire crowd behaves like a viscous fluid (with a parabolic velocity profile). However, if the stiffness level is high enough, the whole crowd behaves like a crystalline solid with a constant velocity profile which only depends on the friction interaction with the walls.

Regarding the parameters of the model, we found that it is possible to reduce the original SFM parameters to three dimensionless parameters. The original parameters interrelate to each other through the dimensionless ones. Many different settings can produce the same dimensionless parameters. Thus, no univocal relations can be established between the individualistic parameters and collective dynamics. In order to explore the outcomes from different dimensionless numbers, we compared numerical results with empirical measurements. We found good candidates to reproduce the qualitative behavior of empirical measurements in the range $0 < \mathcal{K}_c < 68$ with $\mathcal{K} = 685$. Nevertheless, this is a first sketch to arrive at a set of dimensionless parameters that may be suitable to reproduce empirical measurements. We encour-

age further research that seeks to find values of the dimensionless numbers that best reproduce experimental data.

Acknowledgments

This work was supported by the National Scientific and Technical Research Council (spanish: Consejo Nacional de Investigaciones Científicas y Técnicas - CONICET, Argentina) grant Programación Científica 2018 (UBACYT) Number 20020170100628BA.

Appendix A. Reduced-in-units equation of motion

The SFM description in section 3.1 introduces seven parameters (m, τ, v_d, B, A, κ and k_n) attaining for the "individual" behavior of each pedestrian. The collective dynamic, however, requires a smaller set of parameters. In order to identify this smaller set, we introduce the following unit-less magnitudes

$$\begin{cases} t' &= t/\tau \\ r' &= r/B \\ v' &= v/v_d \end{cases} \tag{A.1}$$

The equation of motion (1) can be written in terms of these (unit-less) magnitudes, while only three (reduced) parameters are needed.

$$\frac{d\mathbf{v}'}{dt'} = \hat{\mathbf{e}}_d - \mathbf{v}' + \mathcal{A}\, e^{R'-r'}\, \hat{\mathbf{n}} + g(R'-r') \left[\mathcal{K}\, (\Delta\mathbf{v}' \cdot \hat{\mathbf{t}})\, \hat{\mathbf{t}} + \mathcal{K}_c\, \hat{\mathbf{n}} \right] \tag{A.2}$$

where the smaller set ($\mathcal{A}$,$\mathcal{K}$,$\mathcal{K}_c$) means

$$\mathcal{A} = \frac{A\,\tau}{m\,v_d} \quad , \quad \mathcal{K} = \frac{\kappa\, B\, \tau}{m} \quad , \quad \mathcal{K}_c = \frac{k\, B\, \tau}{m\, v_d} \tag{A.3}$$

Notice that the SFM will arrive to similar collective dynamics whenever the reduced set ($\mathcal{A}$,$\mathcal{K}$,$\mathcal{K}_c$) remains unchanged (although some "individual" parameters are allowed to change). For a deep explanation on the meaning

of the set ($\mathcal{A}$,$\mathcal{K}$,$\mathcal{K}_c$) see section 3.2.

[1] D. Helbing, I. Farkas, and T. Vicsek. Simulating dynamical features of escape panic. Nature, 407:487–490, 2000.

[2] D. Parisi and C. Dorso. Microscopic dynamics of pedestrian evacuation. Physica A, 354:606–618, 2005.

[3] D. Parisi and C. Dorso. Morphological and dynamical aspects of the room evacuation process. Physica A, 385:343–355, 2007.

[4] G. Frank and C. Dorso. Room evacuation in the presence of an obstacle. Physica A, 390:2135–2145, 2011.

[5] Colin M. Henein and Tony White. Macroscopic effects of microscopic forces between agents in crowd models. Physica A: Statistical Mechanics and its Applications, 373:694 – 712, 2007.

[6] J. Fruin. The causes and prevention of crowd disasters. In R.A. Smith and J.F. Dickie, editors, Engineering for Crowd Safety. Elsevier, 1993.

[7] Taras I. Lakoba, D. J. Kaup, and Neal M. Finkelstein. Modifications of the helbing-molnr-farkas-vicsek social force model for pedestrian evolution. SIMULATION, 81(5):339–352, 2005.

[8] Paul A. Langston, Robert Masling, and Basel N. Asmar. Crowd dynamics discrete element multi-circle model. Safety Science, 44(5):395 – 417, 2006.

[9] Peng Lin, Jian Ma, You-Ling Si, Fan-Yu Wu, Guo-Yuan Wang, and Jian-Yu Wang. A numerical study of contact force in competitive evacuation. Chinese Physics B, 26(10):104501, sep 2017.

[10] I. M. Sticco, F. E. Cornes, G. A. Frank, and C. O. Dorso. Beyond the faster-is-slower effect. Phys. Rev. E, 96:052303, Nov 2017.

[11] Rahul Narain, Abhinav Golas, Sean Curtis, and Ming C. Lin. Aggregate dynamics for dense crowd simulation. ACM Trans. Graph., 28(5):122:1–122:8, December 2009.

[12] N. Pelechano, J.Allbeck, and N. Badler. Controlling individual agents in high-density crowd simulation. Proceedings of the 2007 ACM SIGGRAPH/Eurographics Symposium on Computer Animation, pages 99–108, 2007.

[13] Mehdi Moussaïd, Dirk Helbing, and Guy Theraulaz. How simple rules determine pedestrian behavior and crowd disasters. Proceedings of the National Academy of Sciences, 108(17):6884–6888, 2011.

[14] Fernando Alonso-Marroquín, Jonathan Busch, Coraline Chiew, Celia Lozano, and Álvaro Ramírez-Gómez. Simulation of counterflow pedestrian dynamics using spheropolygons. Phys. Rev. E, 90:063305, Dec 2014.

[15] Arianna Bottinelli and Jesse L. Silverberg. How to: Using mode analysis to quantify, analyze, and interpret the mechanisms of high-density collective motion. Frontiers in Applied Mathematics and Statistics, 3:26, 2017.

[16] J. Song, F. Chen, Y. Zhu, N. Zhang, W. Liu, and K. Du. Experiment calibrated simulation modeling of crowding forces in high density crowd. IEEE Access, 7:100162–100173, 2019.

[17] Bachar Kabalan. Crowd dynamics: modeling pedestrian movement and associated generated forces. Theses, Université Paris-Est, January 2016.

[18] A. Jebrane, P. Argoul, A. Hakim, and M. El Rhabi. Estimating contact forces and pressure in a dense crowd: Microscopic and macroscopic models. Applied Mathematical Modelling, 74:409 – 421, 2019.

[19] Litao Wang and Shifei Shen. A pedestrian dynamics model based on heuristics considering contact force information and static friction. Transportmetrica B: Transport Dynamics, 7(1):1117–1129, 2019.

[20] I.M. Sticco, G.A. Frank, F.E. Cornes, and C.O. Dorso. A re-examination of the role of friction in the original social force model. Safety Science, 121:42 – 53, 2020.

[21] Yaouen Fily, Silke Henkes, and M. Cristina Marchetti. Freezing and phase separation of self-propelled disks. Soft Matter, 10:2132–2140, 2014.

[22] Milad Haghani, Majid Sarvi, and Zahra Shahhoseini. When push does not come to shove: Revisiting faster is slower in collective egress of human crowds. Transportation Research Part A: Policy and Practice, 122:51 – 69, 2019.

[23] Dirk Helbing, Anders Johansson, and Habib Zein Al-Abideen. Dynamics of crowd disasters: An empirical study. Phys. Rev. E, 75:046109, Apr 2007.

[24] Rainald Lohner, Britto Muhamad, Prabhu Dambalmath, and Eberhard Haug. Fundamental diagrams for specific very high density crowds. Collective Dynamics, 2, 2018.

[25] Dirk Helbing and Péter Molnár. Social force model for pedestrian dynamics. Phys. Rev. E, 51:4282–4286, May 1995.

[26] Anders Johansson. Constant-net-time headway as a key mechanism behind pedestrian flow dynamics. Phys. Rev. E, 80:026120, Aug 2009.

[27] Meifang Li, Yongxiang Zhao, Lerong He, Wenxiao Chen, and Xianfeng Xu. The parameter calibration and optimization of social force model for the real-life 2013 yaan earthquake evacuation in china. Safety Science, 79:243 – 253, 2015.

[28] Ulrich Weidmann. Transporttechnik der fussgänger. IVT Schriftenreihe, 90, Jan 1992.

[29] S.P. Hoogendoorn and W. Daamen. Microscopic Calibration and Validation of Pedestrian Models: Cross-Comparison of Models Using Experimental Data. In A. Schadschneider, T. Pöschel, R. Kühne, M. Schreckenberg, and D. E. Wolf, editors, Traffic and granular flow '05, volume Part III. Springer, 2007.

[30] A. Seyfried, B. Steffen, W. Klingsch, Th. Lippert, and M. Boltes. The Fundamental Diagram of Pedestrian Movement Revisited - Empirical Results and Modelling. In A. Schadschneider, T. Pöschel, R. Kühne, M. Schreckenberg, and D. E. Wolf, editors, Traffic and granular flow '05, volume Part III. Springer, 2007.

[31] A. Johansson, D. Helbing, and P.K. Shukla. Specification of the social force pedestrian model by evolutionary adjustment to video tracking data. Advances in Complex Systems, 10(supp02):271–288, 2007.

[32] Mehdi Moussaï d, Dirk Helbing, Simon Garnier, Anders Johansson, Maud Combe, and Guy Theraulaz. Experimental study of the behavioural mechanisms underlying self-organization in human crowds. Proceedings of the Royal Society B: Biological Sciences, 276(1668):2755–2762, 2009.

[33] M. Luber, J. A. Stork, G. D. Tipaldi, and K. O. Arras. People tracking with human motion predictions from social forces. In 2010 IEEE International Conference on Robotics and Automation, pages 464–469, May 2010.

[34] Stefan Seer, Christian Rudloff, Thomas Matyus, and Norbert Brändle. Validating social force based models with comprehensive real world motion data. Transportation Research Procedia, 2:724 – 732, 2014. The Conference on Pedestrian and Evacuation Dynamics 2014 (PED 2014), 22-24 October 2014, Delft, The Netherlands.

[35] S. M. P. Siddharth and P. Vedagiri. Modeling the gender effects of pedestrians and calibration of the modified social force model. Transportation Research Record, 2672(31):1–9, 2018.

[36] Arévalo, Roberto and Pugnaloni, Luis A and Zuriguel, Iker and Maza, Diego Contact network topology in tapped granular media. Physical Review E, 87(2):022203, 2013.

[37] Melvin, John W AATD system technical characteristics, design concepts, and trauma assessment criteria. Task EF final report

[38] Zhang, XL and Weng, WG and Yuan, HY and Chen, JG Empirical study of a unidirectional dense crowd during a real mass event Physica A: Statistical Mechanics and its Applications, 392:2781–2791, 2013.

[39] Plimpton, Steve Fast parallel algorithms for short-range molecular dynamics Sandia National Labs,1993